

Military Technical College
Kobry Elkobbah, Cairo,
Egypt.



3rd International Conference
On
Chemical & Environmental
Engineering

HIGH QUALITY DIESEL BY HYDROTREATING GAS OIL OVER MODIFIED TITANIA - SUPPORTED NIMO CATALYSTS.

HANAFI .S. A. * , EL-SYED H. A. * and SOLTAN. E. A. *

ABSTRACT

In this work, methods for preparing alumina-titania and ceria-titania mixed oxide supports were studied. In one method, alumina or ceria were precipitated on the surface of a commercial titanium oxide,. In the second method, alumina or ceria were impregnated on the surface of titania followed by drying and calcination as with the first method .The metal oxide couples used in this study contains NiO and MoO₃. In this study, the catalyst content of NiO is 3 wt% while MoO₃ is 8 wt.% while 89 wt.% is the support material.

Surface area and pore volume measurements for the supports and catalysts were determined. Al, Ce, Ni and Mo contents as well as the coke percentage the spent catalyst were determined by chemical analysis. Characterization of the prepared support samples have been studied by DTA and XRD.

The HDS activities of the prepared catalyst samples have been studied in comparison with titania and alumina catalysts. Two types of catalytic tests were used. One type of measurement was a screening test using the pulse technique while the second type was focused on studying the effect of important process variables as reaction temperature, hydrogen pressure and liquid hourly space velocity (LHSV) on the extent of HDS of gas oil (GO) feedstock and simultaneous HDS and HDN of GO + Pyridine on the selected screened catalysts by using the continuous flow high-pressure fixed bed cata –test unit.

The results revealed that these catalysts are much more active than the conventional NiMo/Al₂O₃ catalysts on HDS and HDN reactions.

The results revealed that these catalysts are much more active than the conventional NiMo/Al₂O₃ catalysts on HDS and HDN reactions. They also demonstrate high aromatic saturation capabilities.

The inhibiting effect of pyridine on gas oil HDS was found to be similar for all catalysts, i.e.: was independent on the support composition. In general, diesel fuel quality improved as the temperature and pressure increased or space velocity decreased.

KEY WORDS

Titania catalysts , Hydrodesulfurization , Hydrodenitrogenation and Diesel improvement.

INTRODUCTION

Support plays an important role in determining nature and number of active sites, and consequently, in the activity of the catalysts. For hydrotreating reactions, γ - Al_2O_3 is the support that is generally used in commercial applications [1]. In order to meet increasingly stringent environmental regulations [2,3] new catalysts are required [5,6]. Several approaches have been applied to achieve the above mentioned goal and variation of support is an important alternative in this direction [7-9]. In order to find out better materials for supporting active components such as Mo and W, a wide variety of materials have been examined for their suitability as supports especially with reference to hydrotreating and related reactions [10,11]. Mixed oxides of various combinations such as TiO_2 - ZrO_2 [12], SiO_2 - TiO_2 [13], TiO_2 - Al_2O_3 [14,15] and ZrO_2 - Al_2O_3 [16] have been investigated. Such extensive investigations revealed that TiO_2 supported molybdenum oxide exhibited about 4.4 times higher activity than the γ - Al_2O_3 supported ones [11]. Several researchers attempted to understand the causes for such outstanding activities [17]. These investigations provided a number of clues towards explaining such high activities. Some of those explanations are: (i) TiO_2 support presents a favorable morphology of MoS_2 ; (ii) TiO_2 support increases the dispersion of active phase; (iii) formation of small crystals of MoS_2 is favorable on TiO_2 support; and (iv) TiO_2 support increases the reducibility and sulfidability of supported phase.

The aim of this work is to evaluate the influence of the addition of oxides (Al_2O_3 , CeO_2) on the physico-chemical characteristics of titania based supports and the corresponding NiMo catalysts and the catalytic performances of the prepared catalysts in HDS of thiophene and GO feedstock. Moreover, experiments in the presence of nitrogen compounds (pyridine added) in the reaction stream were performed in order to analyze the effect of these variables on the performance of the different catalyst formulation.

EXPERIMENTAL

Supports and Catalysts Preparation

Cerium Oxide Support

Cerium oxide support was prepared by the precipitation method [18]. The precipitate was filtered off, washed with deionized water, dried overnight at 120°C and finally calcined at 500°C for 6 h [19].

Mixed Oxide Supports

M- TiO_2 mixed oxide supports (M = Al_2O_3 or CeO_2) were prepared using two different preparation methods: precipitation and impregnation- TiO_2 ($S_{\text{BET}} = 201 \text{ m}^2/\text{g}$, pore volume = $0.38 \text{ cm}^3/\text{g}$) was first calcined at 500°C for 6 h before being used as a support for Al_2O_3 or CeO_2 [20].

Precipitation

Sieved TiO_2 was added to the solution of aluminum nitrate or cerium nitrate. After stirring for one h ammonium hydroxide solution was added until a final pH of 7.5 was

reached. The resulting precipitate was filtered, washed with distilled water. The cake was dried at 120°C over night and then calcined at 500°C for 6 h. Hereafter, these supports were referred as (x) M– Ti where x = 5, 10 and 20 wt % of M [21].

Impregnation

All supports were prepared by adding calcined TiO₂ to a solution of a calculated amount of the metallic salt dissolved in the least amount of H₂O of the required oxide (M) and were dried and calcined at the same conditions as the supports prepared with the first method [22]. Hereafter, these supports was named (x) M /Ti where x represents the nominal of 10 wt.% .The supports (5+5) wt.% / TiO₂ support were prepared by the addition of the required amount of cerium nitrate or aluminium nitrate in two steps (5 wt.% in each one).

The NiO-MoO₃ catalysts were prepared by coimpregnation of the calcined supports (40 x 80 mesh) using the incipient wetness technique. Supports were simultaneous impregnated with an aqueous solution containing the proper amounts of (NH₄)₆Mo₇O₂₄ and Ni(NO₃)₂.6H₂O to obtain catalysts with 8.0 wt.% MoO₃ and 3.0wt.% NiO [23]. The catalysts were then air dried and calcined as mentioned above [24].

Supports and Catalysts Characterization

The surface area and pore volume of the supports and catalysts were determined by the nitrogen adsorption-desorption technique using Micromeritics Gimini 2375 surface area analyzer, and porosity by poresizer 9320 V2-08. The measurements were performed on the oxide form of the samples. Before nitrogen adsorption, samples were heated at 200°C for 2 h in a pure nitrogen flow. Since the average pore sizes of these samples were not large, the mercury penetration method was not valid in the present study. The surface area and pore volume of all the prepared supports and catalysts were determined from the isotherms of N₂ adsorption at -196°C.

The surface area, pore volume and average pore diameter for prepared supports and catalysts are given in Table 1.

The elemental analysis was performed by X-ray florescence method at the Egyptian Geological Survey Mining Authority involving determination of Al and Ce contents in the supports and the Ni and Mo contents of the catalysts. The percentage of carbon was also measured on spent catalysts. The composition of the supports and catalysts is summarized in Table 1.

An X-ray powder diffraction (XRD) was conducted over pure titania without thermal treatment and precalcined at 300°C, 500, 600 °C for 6 h, and also over mixed supports precalcined at 500°C and 600 for 6 h, using Shimadza diffractometer (Type D-D1). The patterns were run with nickel-filtered copper radiation ($\lambda=1.5405 \text{ \AA}$) at 60 kV and 25 mA with scanning speed of 8° in $2\theta \text{ min}^{-1}$ over diffraction angle range. Differential thermal analysis (DTA) was performed, to trace the structure changes accompanying the thermal treatment. This technique was recorded using a thermal analysis apparatus- DTA 50 – of the type Shimadza–50.The sample was ground to

20 meshsize and alumina was used as a reference inert material. All runs were carried out at a heating rate of 10°/min from room temperature up to 800 °C.

Catalytic activity Measurements

Two types of catalytic tests were used. One type of measurement was a screening test using the pulse technique. The second type was focused on studying the effect of important process variables on the extent of sulfur, nitrogen and aromatics removal from the gas oil feedstock (GO) on using the selected screened catalysts in the continuous flow high – pressure fixed bed cata-test unit.

Online Pulse – Reaction

The catalytic functionalities of nickel molybdenum sulfide (NiMoS) catalysts were tested using different model compounds, viz, thiophene for hydrodesulfurization (HDS), cyclohexene for hydrogenation (HYD) and cumene for hydrocracking (HC). In a typical experiment, 0.2 g of a catalyst sample is diluted with inert porcelain of the same particle size as that of the catalyst secured between two plugs of quartz wool inside a stainless steel micro – reactor 10 cm long and 0.8 cm internal diameter. The reaction temperature was controlled within $\pm 0.5^{\circ}\text{C}$ at the given reaction temperatures (250-400°C). The reactor was connected to the injection port of a gas chromatograph (Perkin–Elmer Sigma 3B with FID). For the separation of the reaction effluent of cyclohexene and cumene reaction effluents from the reactor, a packed column 5% Benton 34 + 5% di-isodecylphthalate on a chromosorb W–HP of 80–100 mesh was used. The carrier gas (hydrogen) flow rate was fixed at $20\text{ cm}^3\text{ min}^{-1}$. For thiophene HDS analysis a packed column of 20% silicon oil 200 supported on chromosorb P 80–100 mesh, 8 feet long, was used. Before carrying out the reaction, the catalyst was presulfided at 400°C by injecting 10 μl pulses of 2% dimethyldisulfide (DMDS) in a hydrogen flow [25]. After sulfidation, the temperature was maintained at the reaction temperature. The catalyst was flushed at this temperature by H₂ until no DMDS could be detected in the effluent gas. Reactant under investigation was introduced in micro quantities (1 μL) by the aid of microsyring in the form of pulses.

Continuous flow high – Pressure“Catatest” unit

The gas oil feedstock (b.r.210-348°C) used in this investigation was kindly provided by Cairo Petroleum Refining Company. Its physicochemical characteristics are given in table 2.

The activities of the selected catalysts were measured using two independent tests: HDS of GO in absence of pyridine and simultaneous HDS of GO and hydrodenitrogenation (HDN) of pyridine. The two tests were carried out consecutively (firstly with GO and then with GO enriched with pyridine) on the same catalyst charge and at the same operating conditions. Our investigations were carried out in a down-flow micro reactor unit . The unit consisted mainly of a vertical tubular stainless steel reactor of 19 mm internal diameter and 50 cm long. The reactor was heated in an electric furnace. The catalyst bed was pre-sulfided before starting the reaction runs by treatment with GO previously doped with 2% DMDS which was passed through the catalyst bed at a rate of $30\text{ cm}^3\text{ min}^{-1}$ at 3.0 MPa hydrogen pressure, LHSV of 1.5 h^{-1} and at a constant temperature of 360°C for 6 h [26] The first two hours of

operation were considered as a stabilization period to render the whole unit in steady state operation. The reaction conditions for HDS of GO and for the simultaneous HDS of GO and pyridine HDN tests were carried out at an operating pressure 3.0 - 9.0 MPa, reaction temperature 325 – 425 °C, LHSV 1.5 –6 h⁻¹ and at H₂/Oil ratio of 450v./v.

In all tests, the liquid products (210-348 °C) were analyzed according to ASTM standard methods indicated in table 2.

RESULTS AND DISCUSSION

Catalysts Characteristics

Textural properties

The S_{BET} surface areas, total pore volume v_p and the mean pore diameter of the samples prepared by different methods were determined from the adsorption isotherm of N₂ conducted at -196 °C.

It can be observed that surface areas of samples doped with Ce do not reduce drastically compared to the pure titania. This slight decrease means that incorporation of Ce does not affect texturally titania. Therefore, the catalyst used in this study was prepared using 10 wt.% Ce.

The results obtained are listed in table 1. Inspection of table 1 reveals that the S_{BET} of alumina and ceria containing sample, obtained from the precipitation method, are higher than that of pure titania, indicating the formation of secondary porous system [27].

It can also be seen that the total pore volumes v_p and the average pore diameters of the mixed oxides decrease with increasing the alumina or ceria contents. It is clear from table 1 that the sample 10 wt % M-Ti does not show significant loss of surface area indicating that these samples have a uniform coverage of the porous surface. However, the two stages impregnation of 5 wt.% ((5%+5%) M/Ti), provided a higher average pore diameter than (10 wt.%) M/Ti samples. Possibly, it was due to the different particle size of Al₂O₃ and CeO₂ in the pores of TiO₂.

It is obvious from the results in table 1 that when 3 wt.% NiO and 8 wt.% MoO₃ were impregnated on different supports, the catalyst textural properties were severely affected. For instance, the S_{BET} of the catalyst (10 wt.%) Al-Ti was reduced from 225 m²/g to 150 m²/g when Ni and Mo were impregnated into the support. This drastic decrease of surface area may be due to the blockage of some pores by Ni and Mo since the total pore volume (v_p) of this support was found to decrease from 0.3 cm³/g to 0.2 cm³/g. However, NiMo mixed oxide catalysts presented surface areas between 128–191 m²/g, which are considered good for titania supported catalysts [28]. For all catalysts the surface areas gradually decreased with increasing content of metals (Al, Ce).

X – ray diffraction

The X – ray diffractograms of pure TiO₂ calcined at 500 °C for 6 h. and supported MoO₃ catalysts calcined at the same conditions are presented in Fig. 1. Inspection of Fig. (1-a) reveals that Pure TiO₂ support exists mainly in the anatase form, where the characteristic peak of anatase appears at $2\theta = 25.3^\circ$ [29,30]. Up to 8 wt.% MoO₃ loading, no new peaks due to bulk MoO₃ are observed Fig. (1-b). Samples containing 10 wt.% and above MoO₃, two peaks at $2\theta = 16.5$ and 27.2° were observed which are characterized to crystalline MoO₃ Figs. (1 - c) and (1 - d) It is important to note that the results of XRD study indicate that up to 8 wt. % Mo-loading, MoO₃ remains on the titania support as amorphous phase indicating that MoO₃ is well dispersed into the support and probably as a monolayer [31].

The effect of temperature of calcination of cation – free titania supports was examined in the temperature range of 300 - 600 °C. Calcination of these samples was performed for 6 h at three different temperatures 300, 500 and 600. Fig. 2 shows the XRD of calcined samples and also that of uncalcined TiO₂ for comparison Fig. (2-a).

X-ray patterns of calcined samples at 300 °C show the typical diffraction peak of anatase phase where $2\theta=25.3^\circ$ Fig. (2-b). At higher temperature (i.e. 500°C) diffraction peaks become more intense and narrow due to particle growth. After calcination at 600 °C the anatase phase peaks become less intense, in addition to some peaks of rutile phase observed at $2\theta = 48.1, 55.5$ and 58° which means that anatase was transformed to a more stable phase (rutile) Fig. (2-d).

The same XRD measurements were carried out for Al and Ce – impregnated–titania supports, which are shown in Fig. 3 and 4, respectively.

Abroad characteristic lines belonging to γ -Al₂O₃ appeared clearly for the pure alumina sample at $2\theta = 47.5$ and 66.8° , respectively, (Fig. 3-a), but for Al-impregnated titania sample such lines were not observed. This may be due to the homogeneous dispersion of the alumina in the titania matrix. It is observed from the spectra that anatase is the predominant phase Figure (3-b) and (3-c).

When Ce cations are introduced into the anatase phase, they fill the empty space in the matrix, making the anatase phase more stable (Fig. 4). According to Fig. (4-a), it is clear that the characteristic peaks of CeO₂ are at $2\theta = 27.9, 28.7$ and 47.6° respectively.

The diagram Fig. (4 – b) and (4-c) showed also that the intensity of the peaks of CeO₂ at $2\theta = 27.9, 28.7$ and 47.6° , decreases when CeO₂ is impregnated on titania, confirming that CeO₂ was introduced in the matrix of anatase.

In summary, if XRD spectra of Al and Ce-impregnated-titania supports (Figs. 3 and 4) are compared to cation-free titania support (Fig. 2) we can see that the presence of Al and Ce inhibit or delay the transition of anatase to rutile.

Differential thermal analysis

Fig. 5 represents DTA of Al_2O_3 , (10 wt.%) $\text{Al}_2\text{O}_3/\text{Ti}$, CeO_2 , (10 wt.%) CeO_2/Ti and pure TiO_2 . Inspection of Fig. (5-f) reveals that the commercial TiO_2 contains an endothermic peak at 280.87°C due to the loss of physical adsorbed water. On the contrary, it showed an exothermic behavior around 720°C that should be assigned to a change of the anatase phase to rutile phase. This is in a good agreement with the results of XRD study where the transformation of anatase phase to rutile phase was noticed when TiO_2 was calcined at 600°C .

Alumina had endothermic peaks at about 77.03 and 155.27°C Fig. (5-a) corresponding to the dehydration process, the precursor salt decomposition and the loss of adsorbed water, respectively. Two exothermic peaks were observed at 572.58 and 736.7°C corresponded to the formation of $\gamma\text{-Al}_2\text{O}_3$ and $\kappa\text{-Al}_2\text{O}_3$, respectively [31]. However, these crystallization processes of Al_2O_3 were not seen in the composite oxide.

In case of ceria, a higher temperature (106.13°C) is needed for the dehydration processes. This indicates that CeO_2 contains narrower pores than alumina. Fig. (5-c) showed that CeO_2 had an endothermic peak at 148.12°C corresponding to the precursor salt destructor. Exothermal signal that could be originated in composition of precursor salt still retained in the solid was observed at 185.13°C . This fact suggested partial hydrolysis of the salt at low temperature (148.12°C) synthesis conditions and incomplete condensation reactions. The exothermic behavior at 648.51 and 726.68°C attributed to certain change in the structure Fig (5-c). These crystallization processes of CeO_2 were seen clearly in the composite oxide (10 wt.%) Ce / Ti , which could be assigned to the presence of CeO_2 on the external surface of TiO_2 . Since $\text{Ce} (4+)$ is bigger than $\text{Ti} (4+)$, it fits more tightly into the interstices increasing the stability of the anatase phase.

This result is in a good agreement with the result of textural properties where both values v_p and r of CeO_2 are less than those values for Al_2O_3 .

Catalytic activity measurement Micropulse technique

To analyze the influence of the M (Al or Ce) incorporation method on the activity of NiMo supported on mixed oxides catalyst, we tested the catalysts in three model reactions: thiophene HDS, cyclohexene HYD and cumene HC. Figs. (6, 7) show the influence of reaction temperature on the HDS activity of the prepared catalysts. In general, catalysts prepared from supports containing Al and Ce showed higher activity than pure alumina and ceria catalysts. The lower activity of NiMo/ CeO_2 catalyst is due its low surface area comparable to the other catalysts. This means that a higher amount of molybdenum sulfide may be formed on the other supports than on ceria. In other words, the activity increases with surface area because all catalysts had the same surface concentration of Mo and Ni. Furthermore, a higher activity was obtained on the catalysts with the content of M increasing to 10 wt.%. However, catalysts containing 20 wt.% of the M content show a lower conversion of thiophene, which may be related to the poor textural properties of (20 wt.%) M- Ti support. These results suggest that the highest thiophene HDS conversion in this

system requires an optimum content of M in the mixed supports, which is considered as 10 wt.% in this study. Nevertheless, the way of incorporating M has significant effects on catalytic activity.

It is clear from Fig. 6, 7 that the catalysts prepared by the impregnation method and containing 10 wt.% M-loading possess higher activity than those prepared by precipitation method. However, when 10 wt.% M (Al or Ce) was incorporated in two steps like in the (5+5) M/Ti, catalyst activity of such catalyst was found to be higher than those prepared in one step (Fig. 7). This increase in activity may be attributed to homogeneous dispersion of (Al or Ce) on TiO₂ in case of catalysts prepared by this method [19]. This difference in reactivity among the catalyst can be rationalized in terms of characterization results. In case of the supports prepared by the first method (precipitation), some segregate TiO₂ species were formed i.e. the precipitation caused Al₂O₃ and CeO₂ to occupy some of the surface of TiO₂ [31]. In contrast, when M is incorporated to TiO₂ by impregnation, this certainly produces a support with higher semiconducting character where redox processes such as reduction – sulfidation are improved [32,33]. Moreover, with the second method of preparation (impregnation), an increased level of reaction between the Ti species with the alumina OH's is evidenced by the elimination of a larger amount of the most basic alumina OH's [32]. These findings are reflected in the catalytic performance where NiMo catalysts supported on (10 wt.%)Al/Ti are more active than their NiMo/Al – Ti. Furthermore, when TiO₂ is doped with Ce, the HDS is more accurately correlated with the degree of sulfidation and the ability of creating coordinately unsaturated (CUS) edge/ corner sites responsible for the HDS catalytic activity [34].

It is interesting to note that for HDS and HYD reactions the activities obtained are considerably higher for Al / Ti and Ce / Ti mixed oxide catalysts than alumina and ceria single oxide catalysts Fig. (8) indicating that a synergistic action of the two constituents of the support induced in the supported phase an activity increase which is probably due to metal support interaction [34].

Fig. (8) Also shows that these composite catalysts were found to be very efficient catalysts for hydrogenation of aromatics.

Cumene HC process were used to show the presence of acidity on the supported catalysts. Fig. (8) shows that the order of cumene HC is arranged according to the NiMo supported catalysts as follows:



The high HC activity trend of the catalyst supported on ceria is more accurately correlated with the degree of sulfidation [28]. For alumina supported catalyst, the cumene HC activity can be interpreted in the terms of the presence of acid site at the surface of γ -alumina support [32]. In the case of titania rich catalyst, the acidity should be associated to the metal electron –acceptor character. The acid strength might be affected by any factor which would influence the electronic density in the metal. Furthermore, the sulfidation of titania rich supported catalysts leads to the formation of respective bulk sulfides. The non-stoichiometric nature of these sulfides (i.e., the presence of vacancies) is well known [35]. In that case, anionic vacancies

would have a strong acid strength. Tacking into account these facts are able to explain the existence of an acid strength distribution and to assign the acid properties of these sulfides to the electronic structure of the surface sites (metal and / or vacancies) which in turn also possess coordinative unsaturation. In this sense, since the presence of cationic vacancies modifies the local electronic structure, it also affects the acid strength.

Durability of the selected catalyst samples in thiophene HDS

Fig. (9) represents the thiophene HDS at constant temperature (400⁰C) with successive thiophene injection. From this figure it can be observed that the conversion of thiophene on all catalyst samples showed a higher percentage at the beginning of the experiment and after the injection of some pulses it decreased to a constant conversion percentage. The durability of the selected catalysts decrease in the order:

$$(10 \text{ wt.}\%) \text{ Ce /Ti} > \text{Ti} > (10 \text{ wt.}\%) \text{ Al / Ti} > \text{Ce} > \text{Al}$$

Kraus and Zdrzil [36] have reported that the principle thiophene HDS reaction mechanism over sulfided catalysts proceeds via hydrogenation of the thiophene ring followed by C-S bond scission. They also reported the oligomerization of butadiene with the formation of C₈ and higher hydrocarbons. If a higher concentration of butadiene were to be formed, it is possible that butadiene could interact with the more acidic functionalities of the used catalysts via a carbonium ion mechanism leading to olefin polymerization and pore plugging or surface coverage of active sites [37]. From the above results it can be concluded that the percentage decrease in the catalytic activity is ranging from 13.0 to 23.5 % as shown in Fig. 9.

High Pressure Technique

From the discussion of data presented in the pulse technique, mixed oxides prepared by impregnation method were the most active ones.

In this part the hydrotreatment (HT) of GO was conducted by using four NiMo catalysts. The used supports are: TiO₂, (10 wt.%) Al / Ti, (10 wt.%) Ce / Ti in comparison to Al₂O₃. The main characteristics and chemical composition of these catalyst samples are given in Table 1.

The performance tests were carried out to determine the effectiveness of these catalysts in HDS of GO in absence of pyridine, simultaneous HDS of GO and HDN of pyridine, and HYD activities.

In this section, we discuss the impact of the operating conditions as temperature (325 – 425 °C), pressure (3.0 – 9.0 MPa), LHSV (1 .5 – 6 h⁻¹) at a constant hydrogen to oil ratio of 450 v./v during HDS, simultaneous HDS and pyridine HDN and finally HYD. In particular, we discuss the conversion of sulfur, nitrogen and aromatic compounds, and the selectivity of species i relative to species j, under various operating conditions. Conversion and selectivity are defined as follows:

$$\text{conversion} = \frac{\text{wt.\% of species } i \text{ in feed} - \text{wt.\% of species } i \text{ in product}}{\text{wt.\% of species } i \text{ in feed}}$$

$$\text{Selectivity } (S_{i \text{ to } j}) = \frac{\text{wt.\% of species } i \text{ removed from feed}}{\text{wt.\% of species } j \text{ removed from feed}}$$

where *i* and *j* are sulfur and nitrogen, respectively.

The selectivity considered under HT is the selectivity for sulfur removal and the selectivity for nitrogen removal.

HDS activity for GO in absence of pyridine Effect of reaction temperature

Temperature is normally considered the easiest and most cost-effective means to control the HT process. Increases in temperature normally increase both the rate and conversion of the process [38]. However, the use of excessive temperatures imposes thermodynamic equilibrium constraints on the HT process, which leads to a reduction in conversion [1]. Therefore, it was important to study the effect of temperature on HT within the entire range of temperature considered i.e., 325 – 425°C. All other parameters including the pressure, LHSV and H₂/oil ratio—were kept constant, at values of 5.0 MPa, 1.5 h⁻¹ and 450 v./v., respectively.

Fig. (10) shows the effect of temperature on the conversion of sulfur in the presence of the four catalysts used in this study. It is clear from Fig. 10 that the total sulfur conversion does not change much within the temperature range of 400 – 425°C.

It is clear also from these results that, in general, HDS % increases with increasing temperature. For instance the HDS at 325 °C is 83 % and at 425 °C, it is of the order 98 %.

It is also noticed that the catalyst NiMo/TiO₂ was the best catalyst for the HDS process.

It is important to note that HYD of the gas oil increases with increasing temperature up to 375 °C and above this temperature HYD decrease due to thermodynamic equilibrium.

Therefore, on the study of the effect of other parameters (Pressure, LHSV) on the HDS and HYD this optimum temperature 375 °C was used.

Effect of operating pressure

High operating pressure is one of the effective variables that have a drastic effect on hydrotreating (HT). High hydrogen pressures are known to increase HDS conversion [39] High pressures are also reported to decrease the rate of catalyst deactivation [38]. However, there are limits to which pressure can be used to increase catalyst activity. Sleight [38] reported that an excessive increase in pressure will saturate the catalyst such that any further increase in pressure will not yield the expected corresponding activity. The low capacities of HT reactors also limit the excessive use of pressure, for safety reasons. In the optimization of processes, it is important to operate at pressures that will not only enhance catalyst activity but also be at least possible cost. Therefore, this study was considered to determine the effect of pressure on conversion within the range of pressure selected.

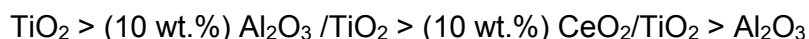
The study covered a pressure range between 3.0 and 9.0 MPa keeping the temperature, LHSV value and H₂/oil ratio constant at 375°C, 1.5 h⁻¹ and 450 v./v., respectively. The pressure-conversion data are presented in Fig. (11). In general the increase of pressure leads to improvement of HDS % and HYD % over all the four used catalysts.

Effect of LHSV

The liquid hourly space velocity (LHSV) is the ratio of the feed volumetric flow rate to the catalyst volume. It gives a measure of how much time lapses while the reactants interact with the catalyst active sites. A reduction in the flow rate could allow for more time for conversion. A reduction in the LHSV value would result in an equivalent decrease in the average reactor temperature that would allow for some conversion to be achieved. As a result, refiners are able to predict how much catalyst will be needed to achieve a certain amount of conversion. A thorough study of the relationship between LHSV and conversion of GO, would contribute much to the optimization of HT process.

Fig. (12) shows the conversion of sulfur compounds against the LHSV value. The LHSV value was varied from 1.5 h⁻¹ to 3 h⁻¹. The temperature, pressure and H₂/oil ratio were also maintained constant at 375°C, 5.0 MPa and 450 v./v., respectively. The conversion of sulfur compounds decrease as the LHSV value increase. By definition, the LHSV is the inverse of the oil contact time with the catalyst, which means that, as the LHSV value increased, the reaction time decreased and conversion was reduced.

In summary, it is recommended that, for maximum HDS, a low LHSV value is recommended. The order of catalytic activities at all operating conditions for HDS is arranged according to the support as follows:



Previous results and new evidence on the role of titania in supported HDS catalysts are analyzed in order to construct a rational explanation for the different findings in Ti-containing HDS catalysts. Some of the important findings follow. TiO₂ is an electronic promoter in HDS catalysts. Ti⁺³ species formed under HDS reaction conditions act as electron donors. These electrons can be easily transferred through the conduction band of the support and be injected to the Mo 3d conduction band. This causes a weakening of the Mo-S bonds and helps the creation of more coordinately unsaturation (CUS) [40]. Murali Dhar et al [41], Pophal et.al. [42] found better sulfidability of molybdenum phases in mixed oxide supported catalyst as compared with an alumina supported one. The smaller crystals of the active phases reported (10 wt.%) Al/Ti and (10 wt.%) Ce/Ti supported catalysts [43]. Zhaobin et al [44] and Cedno et al. [28] reported that TiO₂ increases hydrogen consumption in the experiment. They suggested that TiO₂ reduces the Mo oxidation state by transfer of an electron from Ti to Mo. They also found the weaker metal support interact on mixed oxide supported catalysts. Murali Dhar et al. [41] and Jean-Marie et al. [43] also proposed a similar idea from their oxygen chemisorption experiment. They found that an (10 wt.%) Al/Ti and (10 wt.%) Ce/Ti supported catalysts has more anion vacancies; hence, it absorbs more oxygen. Although there are different

physicochemical properties reported for mixed oxide supported catalysts, it is a general agreement that these mixed oxide supported catalysts have beneficial effects on HT activities. From temperature program reduction (TPR) results Maity et al. [29] and Jean-Marie et al. [43] also observed the presence of a more reducible species in the titanium rich supported catalysts, and it may be reason for showing higher activities.

Simultaneous gas oil HDS and pyridine HDN

It is widely known that organo-nitrogen compounds inhibit HDS reaction. In particular, basic nitrogen species strongly adsorb to the catalyst surface and prevent some HDS reaction from proceeding unless the nitrogen compounds are removed. Even non-basic nitrogen species having low adsorption constants, such as Carbazole, are also known to react in the HT environment to form basic nitrogen. This will inhibit the effectiveness of HDS where the nitrogen compounds reside on the active sites longer than the sulfur compounds, thereby reducing the rate of sulfur extraction [45]

Fig. (13, 14) show the conversion of sulfur and nitrogen compounds against the LHSV value at a pressure of 5.0 and 7.0 MPa. The LHSV value was varied from 1.5 h⁻¹ to 6.0 h⁻¹. The temperature and H₂/oil ratio were also maintained constant at 375°C and 450 v./v., respectively. For both sulfur and nitrogen compounds, the conversion decreased as the LHSV value increased, however, the conversions of sulfur compounds were greater than those of the nitrogen compounds at all LHSV values.

Fig. (15) also shows an increase in the selectivity for sulfur reduction relative to nitrogen as LHSV value increases. This condition suggests a faster HDS process, compared to HDN, and confirms the fact that HDN requires a longer time to occur, because it goes through two reaction steps of hydrogenation and denitrogenation. At low LHSV values, the selectivity for nitrogen removal increases, which leads to lower selectivities for sulfur removal.

High hydrogen pressures are known to increase both HDS and HDN conversion. As the pressure increases, the selectivity for nitrogen removal increases, relative to that for sulfur removal. This result is because an increase in pressure increases the rate of hydrogenation, which leads to increased HDN. The selectivity for sulfur removal decreases, because the predominant path for HDS is the direct sulfur extraction, meaning that pressure increases do not have much effect on HDS compared to that on HDN.

The activities for HDS and HDN increased over rich and pure-TiO₂ based catalysts due to an improvement in reducing and sulfiding of molybdena over TiO₂ supported catalysts than those supported on alumina [46]. This decrease in the activity of the alumina catalyst was related to a loss of nickel in the amorphous Al₂O₃ [47].

Effect of process conditions on aromatics content and diesel index

A high aromatic content in diesel fuel will result in high particle emission and low diesel index of the fuel [48]. For particle emission control and diesel index improvements, it is important to reduce the aromatic content of the diesel fuels.

Another aspect concerns the inhibiting effect of aromatic compounds present in the feed, where aromatics may compete with sulfur compounds in the adsorption or reaction processes [49]. Therefore, this study was conducted to determine how the operating conditions affect the aromatic conversion and diesel index of GO.

Fig. (16-18) illustrate the effects of temperature, pressure and LHSV on the aromatic content of GO. Aromatics are converted to saturates as the pressure and temperature increase and as LHSV decrease. At low to moderate pressures (3.0-5.0 MPa), there is a sharp decrease in the aromatic content, and however, this value reduces with further increases in pressure (5.0-7.0 MPa). However, at the higher pressure (7.0-9.0 MPa), this value reduces and approaches equilibrium. Equilibrium is approached faster as the temperature increases to 375°C. This is because, generally in this temperature region, aromatics hydrogenation is kinetically controlled and an increase in temperature, increases the rate of forward reaction, resulting in a higher conversion of aromatics. However, at higher temperatures, thermodynamic effects dominate, thus leading to a shift in equilibrium in favor of the reverse reaction (dehydrogenation), which results in more aromatics being produced in the hydrotreated products and HYD passing through a minimum [45].

Diesel index increases with increasing temperature up to 375°C. Further increase of temperature gives drops of this value, due to the reaction equilibrium shifts towards dehydrogenation. (Fig. 19) Increasing operating pressure increases diesel index value due to enhancing aromatics removal (Fig. 20), whereas the increase of LHSV decreases diesel index due to decreasing the contact time of the reaction (Fig. 21).

Catalyst deactivation

The percentage of carbon was measured on spent catalysts. The spent catalysts were washed with hot toluene by the soxhlete process and dried at 110 °C before carbon analysis. Coke is defined in this work as being the carbon content on spent catalysts. The tendency of the catalysts to accumulate more coke percent can be arranged as follows:

$$\text{Al} > (10 \text{ wt.}\%) \text{ Al} / \text{Ti} > \text{Ti} > (10 \text{ wt.}\%) \text{ Ce} / \text{Ti}$$

Where the weight percentage of coke on the catalysts after HT of GO are 1.58, 1.41, 1.05 and 0.94 wt% on the NiMo catalyst supports; Al, (10 wt.%) Al / Ti, Ti and (10 wt.%) Ce / Ti, respectively. Alumina supported catalyst have acidic sites [38] that enhance cracking of heavy molecules and intermolecular hydrogen-transfer reaction between adsorbed alkyl aromatic species. NiMo/Al₂O₃ catalyst also has the largest pore diameter (Table 1) and it may facilitate coke deposition into the pore cavity. Pore size of a catalyst plays an important role in controlling of coke formation.

The pore not only gives the path of the reactant and product molecules but also is the site for deactivation. Coke deposition has an adverse effect on the catalyst porosity. The mode of catalyst deactivation depends on pore diameter. For a small pore diameter, catalyst deactivation occurs due to mouth plugging, whereas for a large pore diameter, the catalyst is deactivated by the core poisoning [42]. Also coke deposition depends inversely on the hydrogenation activity of the catalyst, i. e.; the amount of coke deposited depends on the hydrogenation properties of the catalyst.

CONCLUSIONS

The main conclusions that may be drawn from this study could be summarized as follows:

- The NiMo – Mixed oxide catalysts presented surface area between 128 – 191 m²/g which may be considered to be good for titania supported catalysts.
- The XRD study showed that TiO₂ support exists mainly in the anatase form and at high temperature (600-700C°) it is transferred to the rutile form as confirmed from the DTA.
- The XRD of pure Alumina showed the lines characteristic of γ -Al₂O₃ but for Al-impregnated titania, these lines disappear and the peaks of TiO₂ (anatase) was observed. This may be due to homogeneous dispersion of alumina in titania matrix.
- The addition of CeO₂ to TiO₂ was found to have similar effect on the texture of TiO₂. It can be concluded that the presence of Al₂O₃ or CeO₂ inhibit or delay the transition of anatase to rutile.
- The addition of MoO₃ to TiO₂ does not affect the textural structure of TiO₂ up to 8.0 wt.% MoO₃ loading, but above this value the lines of MoO₃ oxide were observed in the XRD pattern indicating that in samples with low MoO₃ (up to 8.0 wt.%), MoO₃ remains on titania support as an amorphous phase indicating that MoO₃ is well dispersed into the support.
- In general catalysts prepared from supports containing Al or Ce showed higher activity than pure alumina and ceria. The lower activity of NiMo/CeO₂ catalyst is due to the low surface area compared to the other catalysts.
- The catalysts prepared by the impregnation method and containing 10.0 wt.% Al₂O₃ or CeO₂ loading posses higher activity than those prepared by the precipitation method indicating homogeneous dispersion of Al or Ce in case of the first series of catalysts.
- The composition of supports have a pronounced effect on the HDS of GO and the simultaneous HDS and HDN of GO + pyridine where the catalyst activities were found to follow the order:
 - Ti > (10 wt.%) Al / Ti > (10 wt.%) Ce / Ti > Al
- The diesel fuel quality, sulfur, nitrogen and aromatics content, diesel index and specific gravity were improved as temperature and pressure increase and as LHSV decreases. The deactivation is observed for the catalyst which has higher coke deposition tendencies. Coke is high on alumina support catalyst.

REFERENCES

- [1] Whitchurst, D. D.; Isoda, T. and Mochida, I. *Adv. Catal.* Vol. 42, p.345 (1998).
- [2] Song, C. S. *Catal. Today*, vol. 86, 211 (2003).
- [3] Song, C. S. and Ma, X. L. *Appl. Catal. B: Environ.* Vol. 41, 207 (2003).
- [4] Babich, I. V. and Moulijn, J. A. *Fuel* vol. 82, p. 607 (2003).
- [5] Jeremy, G. *World Refining* vol. 14 (6), p.22 (2004).
- [6] Oyama, S. T. *J. Catal.* Vol. 216, p. 343 (2003).
- [7] Kabe, T.; Aoyama, Y.; Wang, D.; Ishihara, A.; Qian, W.; Hosoya, M. and Zhang, Q. *Appl. Catal. A: vol.* 209, p.237 (2001).
- [8] Oyama, S. T.; Wang, X.; Lee, Y. K.; Bando, K. and Requejo, F. G. *J. Catal.* Vol.210, p.207 (2002).
- [9] Stinner, C.; Prins, R. and Weber, T. *J. Catal.* Vol. 202, p.187 (2001).
- [10] Kim, J. H.; Ma, X. and Song, C. *Energy & Fuels.* Vol.19 , p.353 (2005).
- [11] Breyse, M.; Afanasiev, P.; Geantet, C. and Vrinat, M. ,*Catal. Today*, vol.86,p5,(2003).
- [12] Barrera, M. C.; Viniegra, M.; Escobar, J.; Vrinat, M.; de los Reyes, J. A.; Murrieta, F. and Garcia, J., *Catal. Today* vol.98,p131,(2004).
- [13] Reddy, B. M.; Chowdhury, B. and Smirniotis, P. *Appl. Catal. A: vol.* 21, p.19 (2001).
- [14] Grzechowiak, J.; Rynkowski, J. and Wereszako, I. *Catal. Today* vol. 65, p. 225 (2001).
- [15] Segawa, K.; Takahashi, K. and Satoh, S. *Catal. Today.* Vol. 63, p.123 (2000).
- [16] Li, G.; Li, W.; Zhang, M. and Tao, K. *Appl. Catal. A: vol.* 273, p. 233 (2004).
- [17] Maity, S. K.; Rana, M. S.; Bej. S. K.; Ancheyta- Juarez, J.; Dhar, G. M. and Parasada, T. S. R. *Appl. Catal. A: vol.* 205, p. 215 (2001).
- [18] Chen, Y. W. and Tsai, M. C. *Ind. Eng. Chem. Res.* Vol.36,p2521,(1997).
- [19] Kunisada, N.; Choi, K. H.; Korai, Y.; Mochida, I. and Nakano, K. *Appl. Catal. A: vol.* 276, p.51 (2004).
- [20] Choi, K. H.; Kunisada, N.; Korai, Y.; Mochida, I. and Nakano, K. ,*Catal. Today* vol.86,p277,(2003).
- [21] Zhaobin, W.; Qin, X.; Xiexian, G.; Sham, E. L.; Grange, P. and Delmon, B. *Appl. Catal.* Vol. 63, p. 305 (1990).
- [22] Quartararo, J.; Mignard, S. and Kasztelan, S. *J. Catal.* Vol. 192, p.307 (2000).
- [23] Isoda, I.; Nagao, S.; Ma, X.; Korai, Y. and Mochida, I. *Energy& Fuels* vol.10, p.1078 (1996).
- [24] Ramirez, J.; Contreras, R.; Castillo, P.; Klimova, T.; Zarate, R. and Luna, R. *Appl. Catal. A: vol.* 197, p. 69 (2000).
- [25] Sarbak, Z. *Catal. Today* vol. 65 (2-4), p. 293 (2001).
- [26] Michoud, P.; Lemberton, J. L. and Perot, G. *Appl. Catal. A: vol.*169, p.343 (1998).
- [27] Jan, M.; Marek, L. and Florian, D. *Catal. Lett.* Vol. 51, p. 65 (1998).
- [28] Cedeno, L.; Zanella, R.; Ramirez, J.; Mendoza, H.; Hernandez, G. and Schacht, p., *Catal. Today* vol.98,p83,(2004).
- [29] Maity, S. K.; Ancheyta, J. and Rana, M. S. *Energy & Fuels* vol. 19, p.343 (2005).
- [30] Dzwigaj, S.; Louis, C.; Breyse, M.; Cattenot, M.; Bellier, V.; Geantet, C.; Vriant, M.; Blanchard, P.; Payen, E.; Inous, S.; Kudo, H. and Yoshimura, Y. *Appl. Catal. B: vol.* 41, p.181 (2003).

- [31] Guoran, L.; Wei, L.; Minghui, Z. and Keyi, T. *Catal. Today* vol. 93 – 95, p.595 (2004).
- [32] Arrouvel, C.; Breyse, M.; Toulhoal, H. and Raybaud, P., *J. Catal.* Vol.232,p 161,(2005)
- [33] Shimada, H. *Catal. Today* vol. 86, p. 17 (2003).
- [34] Rana, M. S.; Srinivas, B. N.; Maity, S. K.; Murali Dhar, G.; Prasad Rao, T. S. R. In: Delmon, B.; Froment, G. F. and Grany, P (Eds.). *Stud. Surf. Sci. Catal.* Vol.127, p.327 (1999).
- [35] Chary, K. V. R.; Vijayakumar, V.; Kanta Rao, P.; Nosov, A. V. and Mastikhin, V. *M. J. Mol. Catal. A: vol.96,pls,(1995).*
- [36] Kraus, J. and Zdrasil, M. *React. Kinet. Catal. Lett.* Vol. 6, p. 475 (1977).
- [37] Daly, F, P.; Ando, H.; Schmitt, J. L. and Sturm, E. A. , *J. Catal.* Vol.108,p401,(1987).
- [38] Speight, J. G. *The desulfurization of Heavy Oils and Residua*; Marcel Dekker: New York, (2000).
- [39] Girgis, M. J. and Gates, B. C. *Ind. Eng. Chem. Res.* Vol. 30, p.2021 (1991).
- [40] Ramirez, J.; Macias, G.; Cedeno, L.; Gutierrez-Alejandr, A.; Cuevas, R. and Castillo, P. *Cata. Today* vol. 98 (1-2), p. 19 (2004).
- [41] Murali Dhar, G.; Srinivas, B. N.; Rana, M. S.; Kumar, M. and Maity, S. K. *Catal. Today* vol. 86, p. 45 (2003).
- [42] Pophal, C.; Kameda, F.; Hocino, K.; Yoshinaka, S. and Segawa, K. *Catal. Today*, vol,39 p. 21 (1997).
- [43] Jean - Marie, H.; Hoang - van, C.; Lucic, D. and Rondronirina, H. J. *Catal.* Vol. 157 (2), p.361 (1996).
- [44] Zhaobin, W.; Qin, X.; Xienxian, G.; Sham, E. L.; Grange, P. and Delmon, B. *Appl. Catal* vol.75, p.179 (1991).
- [45] Abena, O. B.; Ajay, K. D.; Deena, F. and John, A., *Ind. Erg. Chem. Res.*, vol. 44, p 7935, (2005) .
- [46] Wei, Z. B.; Xin, Q. and Xiong, G. *Catal. Lett.* Vol. 15, p.255 (1992).
- [47] Olguin, E.; Vrinat, M.; Cedeno, L.; Ramirez, J.; Borque, M. P. and Lopez Agudo, A. *Appl. Catal. A: vol. 165, p.1 (1999).*
- [48] Jack, P. *World Refining* vol. 15 (2) p. 40 (2005).
- [49] Georgina, C. L.; Ricardo, S – M.; Maria, C. M.; Jesus, C. and Jose, L. C. *Fuel* vol. 83, p. 1381 (2004).

Table (1): Textural Properties of Supports and Catalysts.

Carrier (Support)			
Composition	Surface area, m²/g	Pore volume, cm³/g	Average pore diameter, A^o
Single oxide support			
TiO ₂ ^c	201	0.38	75.6
Al ₂ O ₃ ^d	200	0.57	114.0
CeO ₂	70.0	0.124	70.9
Mixed oxide supports prepared by precipitation			
(5%) Al ₂ O ₃ - TiO ₂	242	0.36	64.5
(10%) Al ₂ O ₃ - TiO ₂	225	0.30	53.3
(20%) Al ₂ O ₃ - TiO ₂	210	0.20	38.0
(5%) CeO ₂ - TiO ₂	226	0.27	47.8
(10%) CeO ₂ - TiO ₂	215	0.25	46.5
(20%) CeO ₂ - TiO ₂	208	0.20	38.5
Mixed oxide supports prepared by impregnation			
(10%) Al ₂ O ₃ - TiO ₂	170	0.29	68.2
(5+5%) Al ₂ O ₃ - TiO ₂	168	0.31	73.8
(10%) CeO ₂ - TiO ₂	194	0.23	47.4
(5+5%) CeO ₂ - TiO ₂	193	0.24	49.7
Catalyst ^a			
Designation	Surface area, m²/g	Pore volume, cm³/g	Average pore diameter, A^o
Ti	90.98	0.25	110.0
Al	138	0.45	130.4
Ce	38.68	0.084	86.9
(5%) Al- Ti	160.0	0.23	57.5
(10%) Al- Ti	150.37	0.20	53.2
(20%) Al- Ti	143.85	0.17	47.3
(5%) Ce-Ti	191.0	0.18	37.7
(10%) Ce-Ti	180.0	0.16	35.6
(20%) Ce-Ti	170.0	0.12	28.2
(10%) Al/ Ti	130.0	0.19	58.5
(5+5%) Al/Ti	128.0	0.20	62.5
(10%) Ce/Ti	165.0	0.15	36.4
(5+5%) Ce/Ti	162.0	0.16	39.5

A = The active metal oxide MoO₃ = 8.0 wt% and the promoter NiO = 3.0 wt%

b = Average pore diameter from; $4 \text{ (pore volume / BET surface area)}$.

c = Commercial titania (Norton Co. USA)

d = Commercial alumina, SA673 (Norton Co. USA).

Table 2. Physicochemical Properties of GO Feedstock.

Properties	Value	Method
Specific Gravity 60/60 °f	0.8274	ASTM D 289-65
°API Gravity	39.52	ASTM D 287-92
Refractive Index, 20°C	1.4634	ASTM D1218-92
Molecular Weight	210	ASTM 2503-82
Pour Pint, °C	-3	ASTM D97-88
Aniline Point, °C	69	ASTM D611-82
Diesel Index	62	Calculated from measured aniline point and °API gravity
Specific Color	0.5	ASTM D1500
C, wt %	86.3	
H, wt %	13.2	
Sulfur Content, wt %	0.46	ASTM D4294-90 (x-ray fluorescence)
Nitrogen Content, wt%	0.02	Frigle-deumes method.
Aromatics Content, wt%	25.0	Silica gel column
ASTM Distillation, Vol. %, °C		ASTM-D2887
IBP	210	
10 %	248	
50 %	287	
90 %	311	
EP	348	

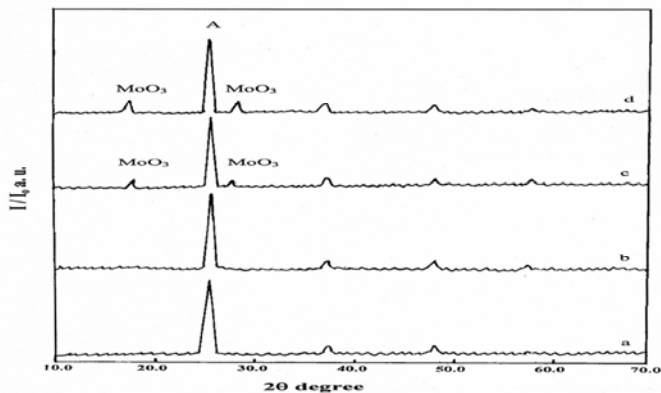


Fig. 1: X-ray diffractograms of MoO₃/TiO₂ Catalysts:
 (a) = pure TiO₂,
 (b) = 8 wt. % MoO₃/TiO₂,
 (c) = 10 wt% MoO₃/TiO₂ and
 (d) = 12 wt% MoO₃/TiO₂

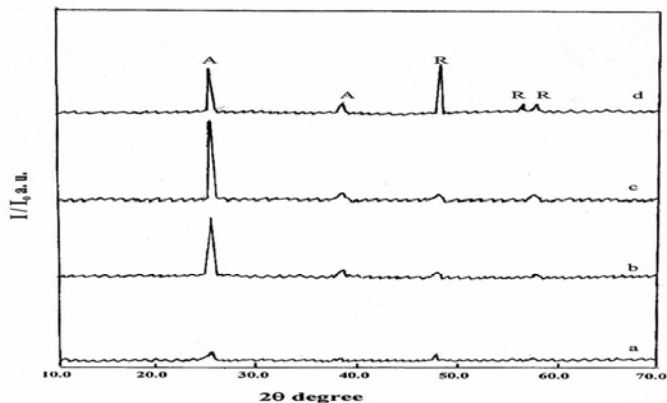


Fig. 2: X-ray diffractograms of Cation – free Titania:
 (a) = Without Treatment,
 (b) = Calcined at 300 °C,
 (c) = Calcined at 500 °C and
 (d) = Calcined at 600 °C.

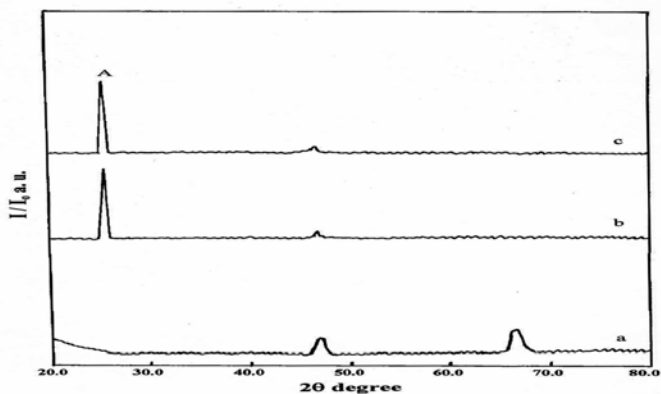


Fig. 3: X-ray diffractograms of:
 (a) = Al₂O₃ at 500 °C,
 (b) = (10 wt%) Al/Ti at 500 °C,
 (c) = (10 wt%) Al/Ti at 600 °C.

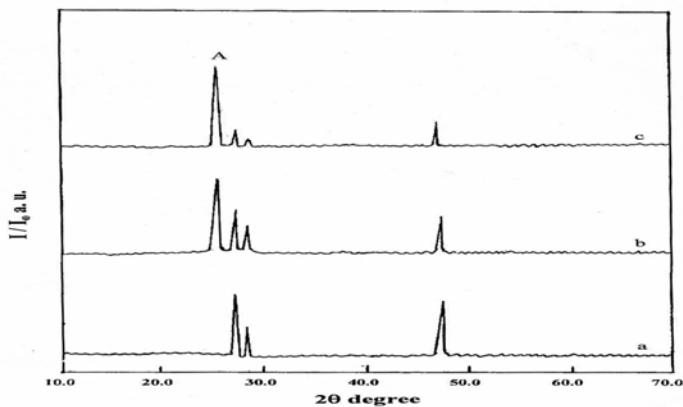


Fig. 4: X-ray diffractograms of:
 (a) = CeO₂ at 500 °C,
 (b) = (10 wt%) Ce/Ti at 500 °C,
 (c) = (10 wt%) Ce/Ti at 600 °C.

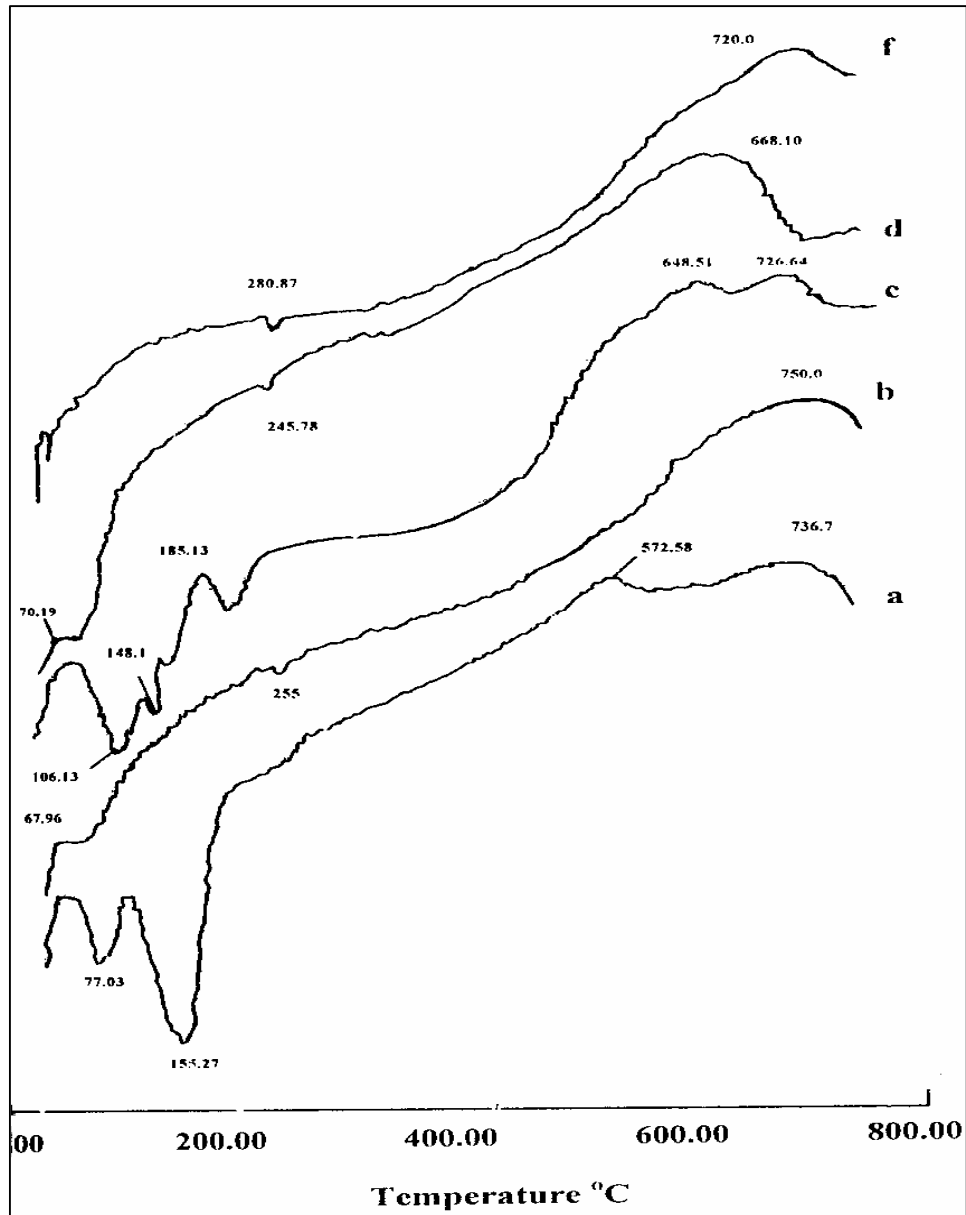


Fig. 5: DTA Curve of; (a) = Al₂O₃, (b) = (10 wt.% Al/Ti, (c) = (Ce O₂ (d) = (10 wt%) Ce / Ti and (f) = TiO₂

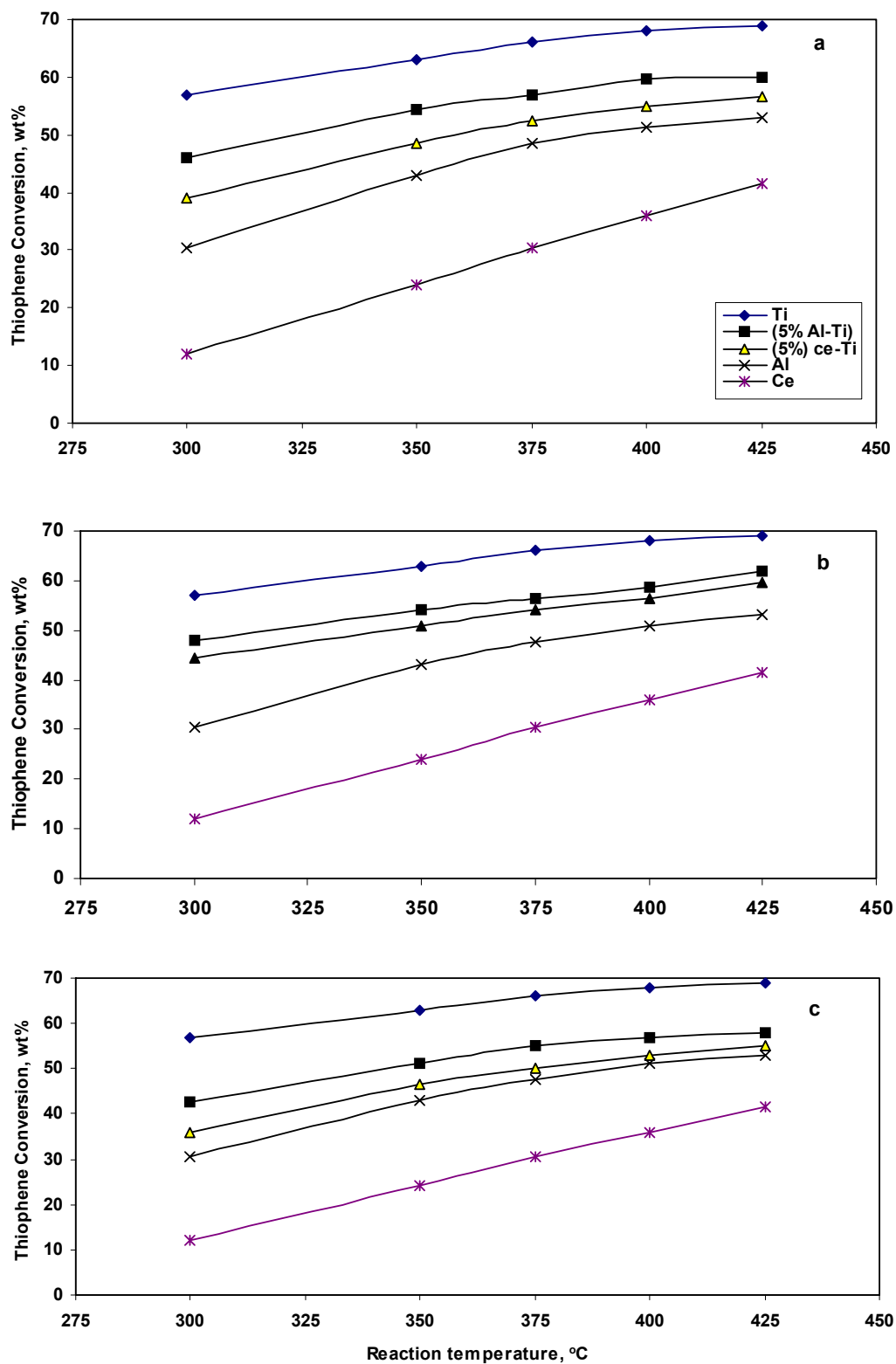


Fig. 6 : Thiophene conversion as a function of reaction temperature on catalysts prepared by M precipitation (M= Ce or Al): a = 5 wt%, b= 10 wt% and c = 20 wt%

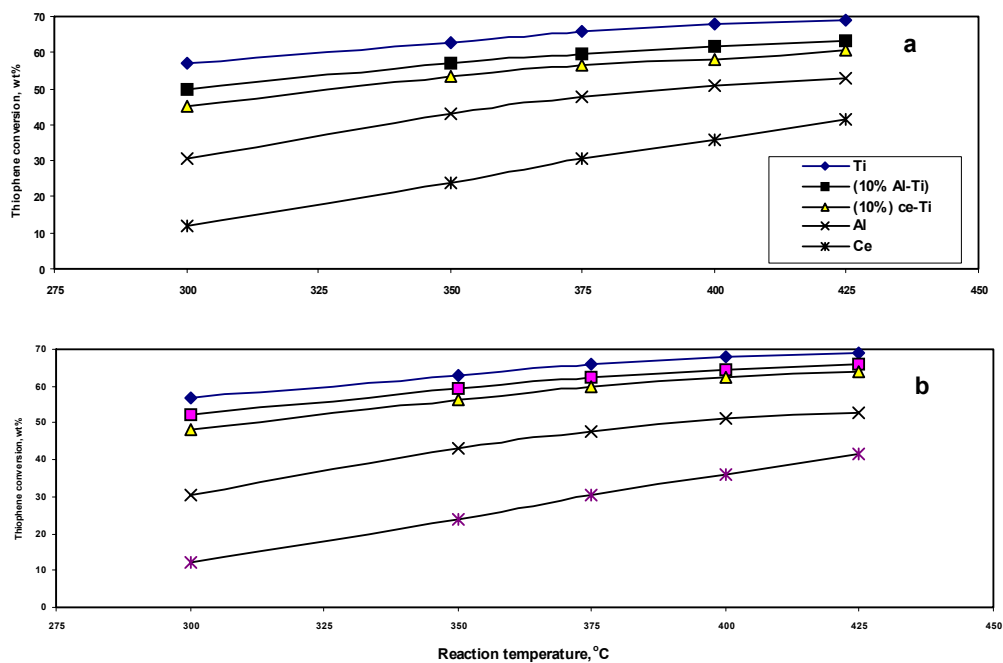


Fig. 7 : Thiophene conversion as a function of reaction temperature on catalysts prepared by M impregnation (M= Ce or Al): a = 10 wt%, b= (5+5) wt%

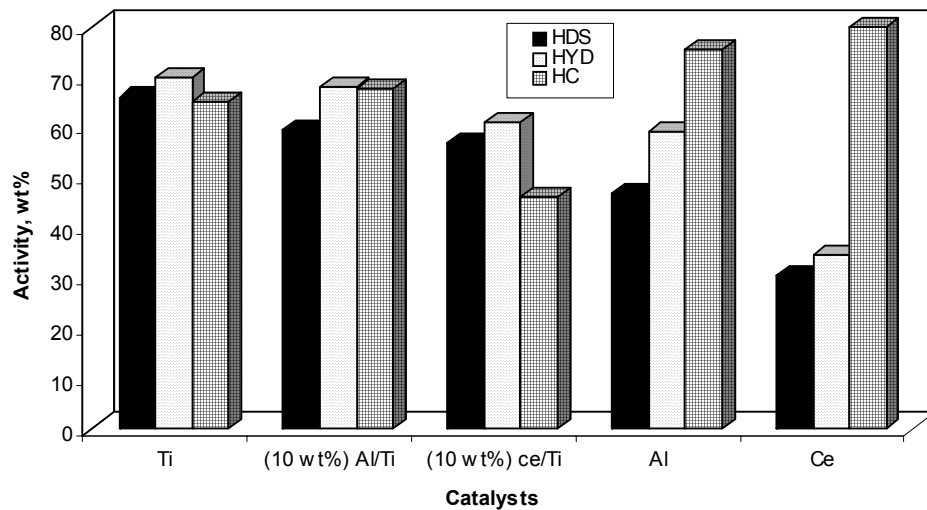


Fig. 8: Effect of support on catalytic activity for various functionalities at 375°C

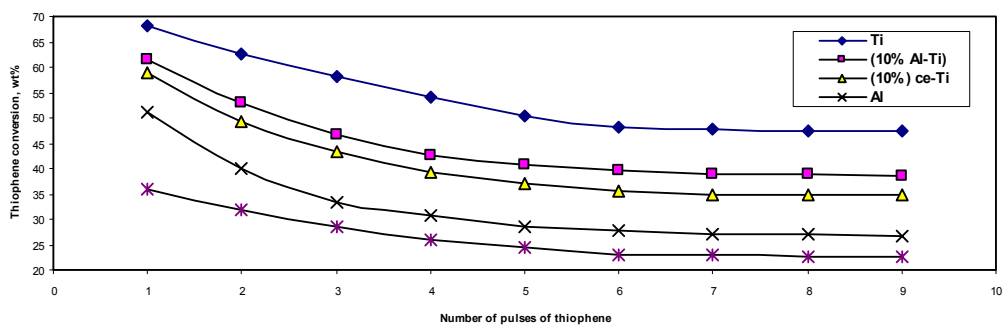


Fig. 9: Durability of catalyst samples at 400°C

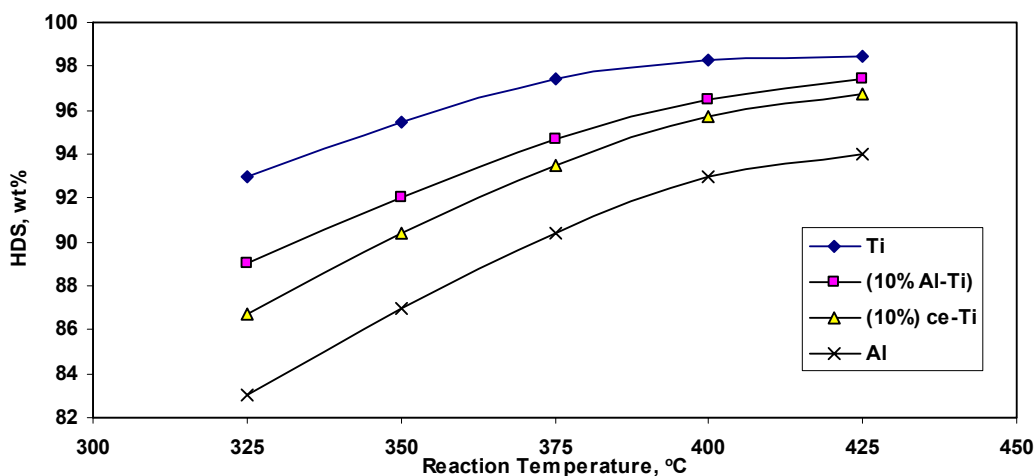


Fig. 10: HDS of diesel fuel product (210 - 348°C) as a function of reaction temperature (pressure = 5.0 MPa, LHSV = 1.5 h⁻¹ and H₂/Oil Ratio = 450 v./v.)

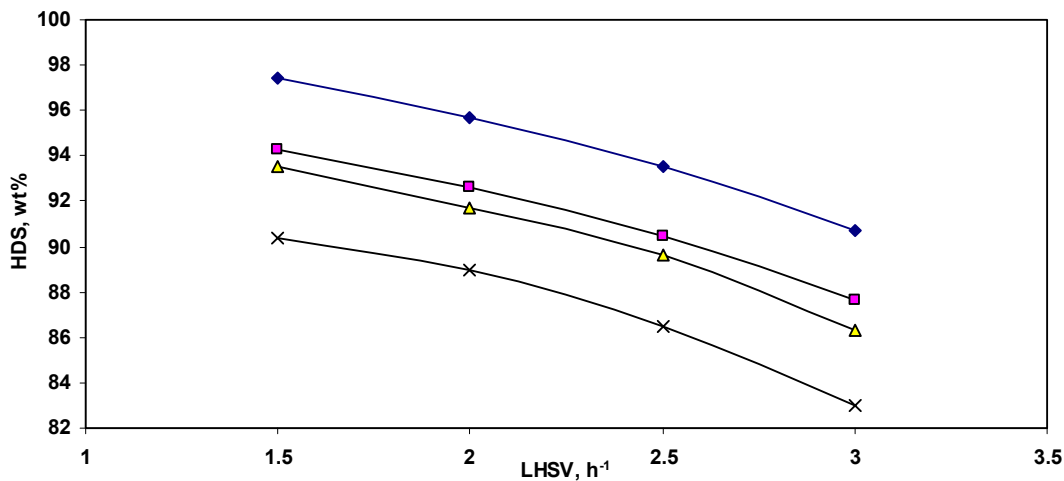


Fig. 11: HDS of diesel fuel product (210-348°C) as a function of operating pressure (Temperature = 375°C, LHSV = 1.5 h⁻¹ and H₂/Oil Ratio = 450 v./v.)

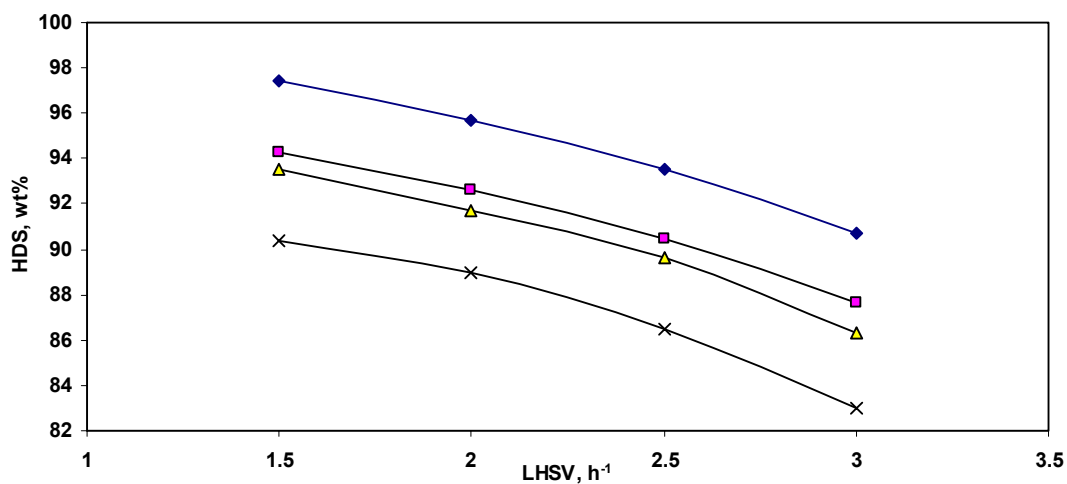


Fig. 12: HDS of diesel fuel product (210 - 348°C) as a function of LHSV (Temperature = 375°C, Operating pressure = 5.0 MPa and H₂/Oil Ratio = 450 v./v.)

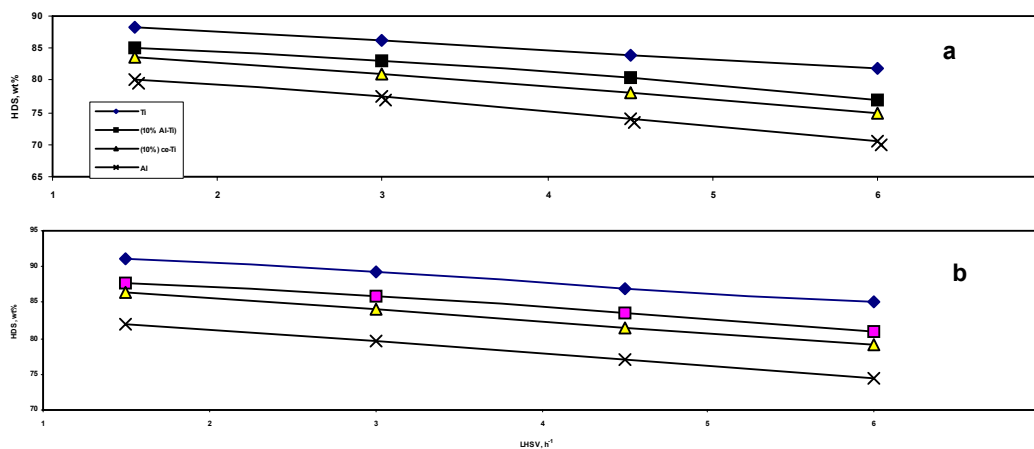


Fig. 13: HDS of diesel fuel product (210 - 348°C) as a function of LHSV: (a) P=5.0, (b) P= 7.0MPa

(Temperature = 375°C, Pressure = 7.0 MPa and H₂/oil Ratio = 450 v./v. and Total Nitrogen = 0.82wt)

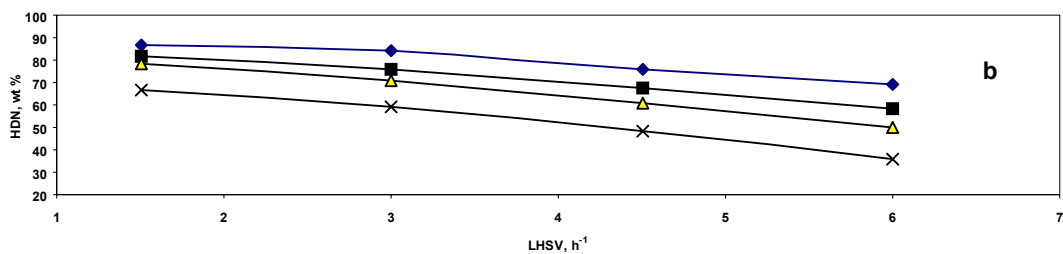


Fig. 14: HDN of diesel fuel product (210 - 348°C) as a function of LHSV (a) P= 5.0MPa, (b) P= 7.0 MPa

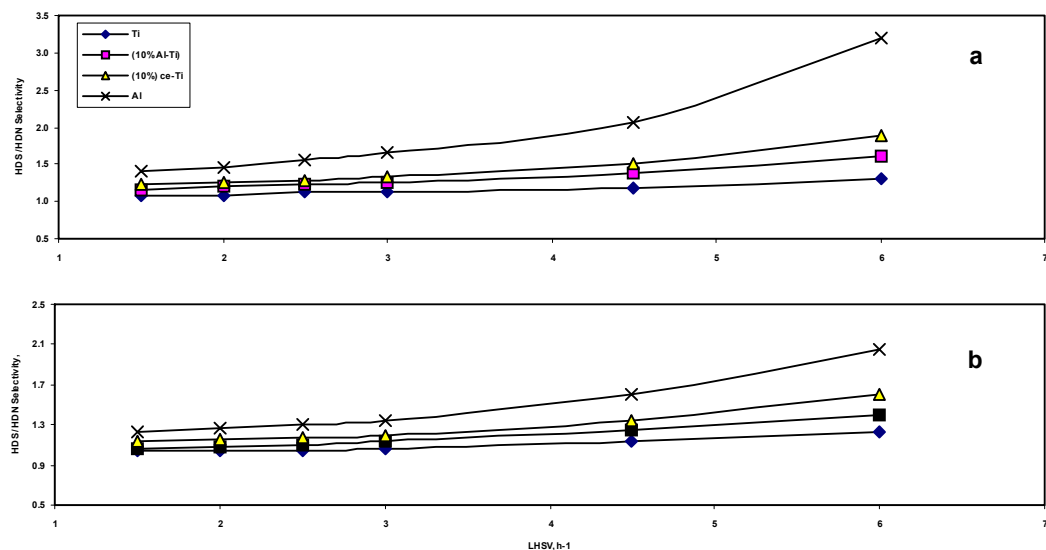


Fig. 15: HDS/HDN selectivity of diesel fuel product (210-348°C) a function of LHSV: (a) P= 5.0MPa, (b) P=7.0 MPa (Temperature = 378°C, H₂/Oil Ratio = 450 v./v. and Nitrogen = 0.82 wt%)

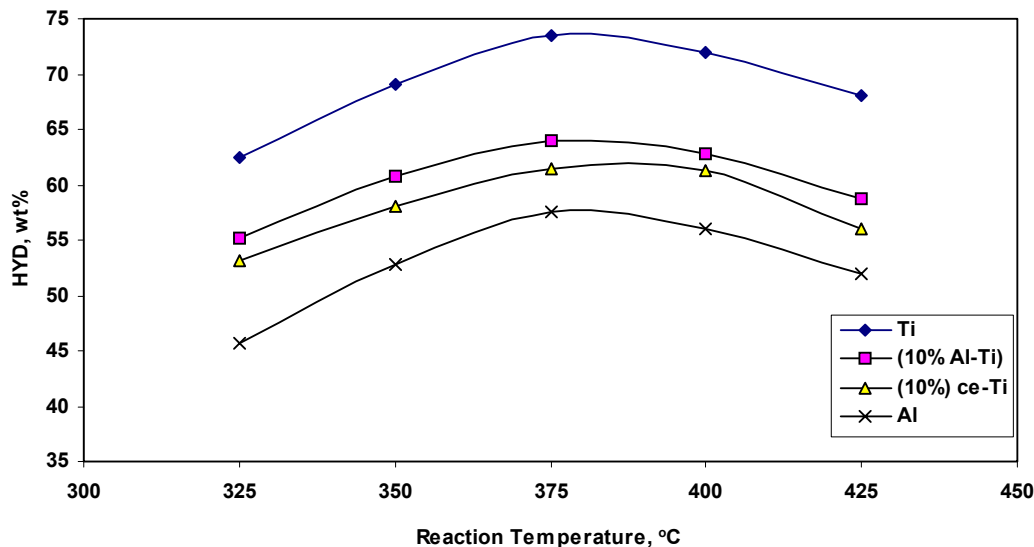


Fig. 16: Aromatics removal of diesel fuel product (210-348°C) as a function of reaction temperature (pressure = 5.0 MPa, LHSV = 1.5 h⁻¹ and H₂/Oil Ratio = 450 v./v.)

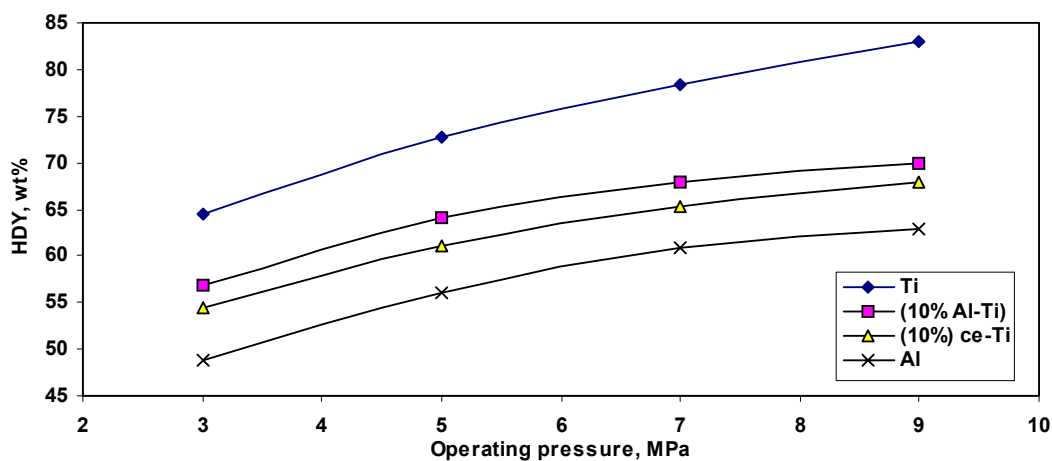


Fig. 17: Aromatics removal of diesel fuel product (210-348°C) as a function of operating pressure

(Temperature = 375 °C, LHSV = 1.5 h⁻¹ and H₂/Oil Ratio = 450 v./v.)

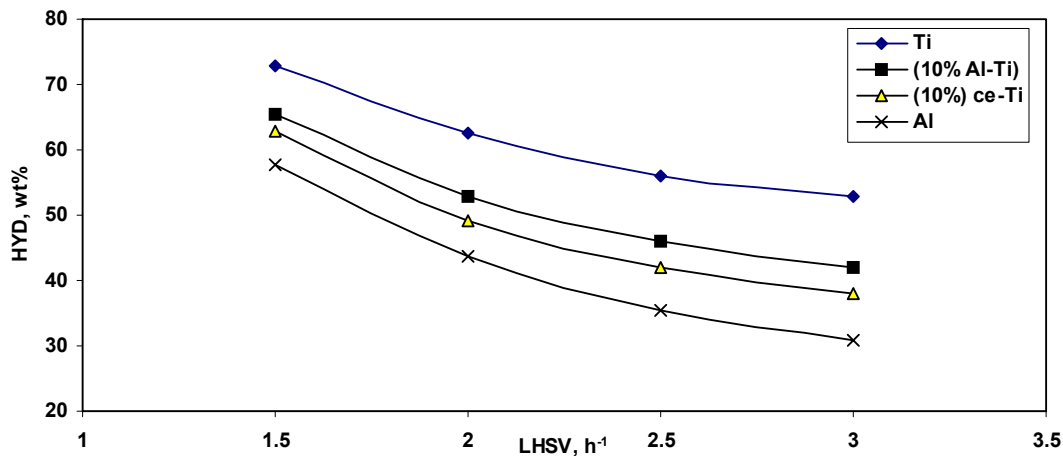


Fig. 18: Aromatics removal of diesel fuel product (210-348°C) as a function of LHSV

(Temperature = 375 °C, Operating Pressure = 5.0 MPa and H₂/Oil Ratio = 450 v./v.)

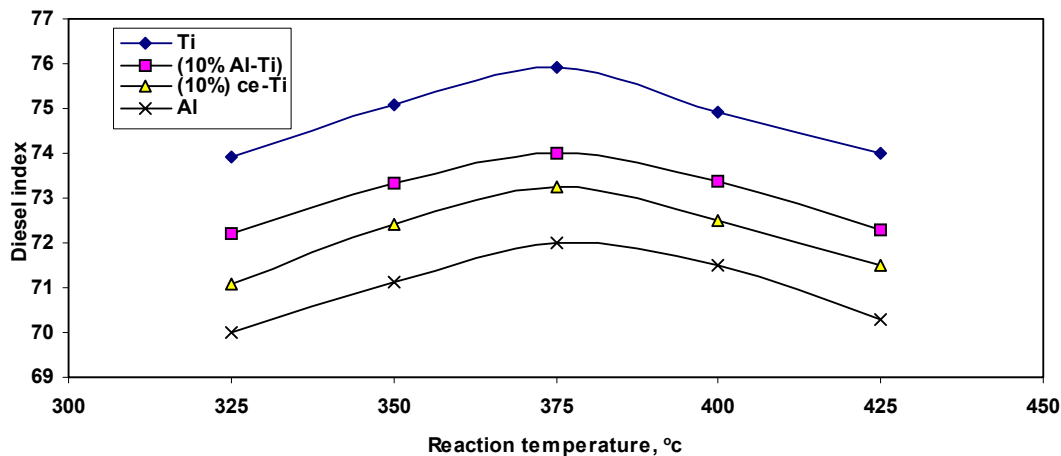


Fig. 19: Diesel index of diesel fuel product (210-348°C) as a function of reaction temperature

(Pressure = 5.0 MPa, LHSV = 1.5 h⁻¹ and H₂/oil Ratio = 450 v./v.)

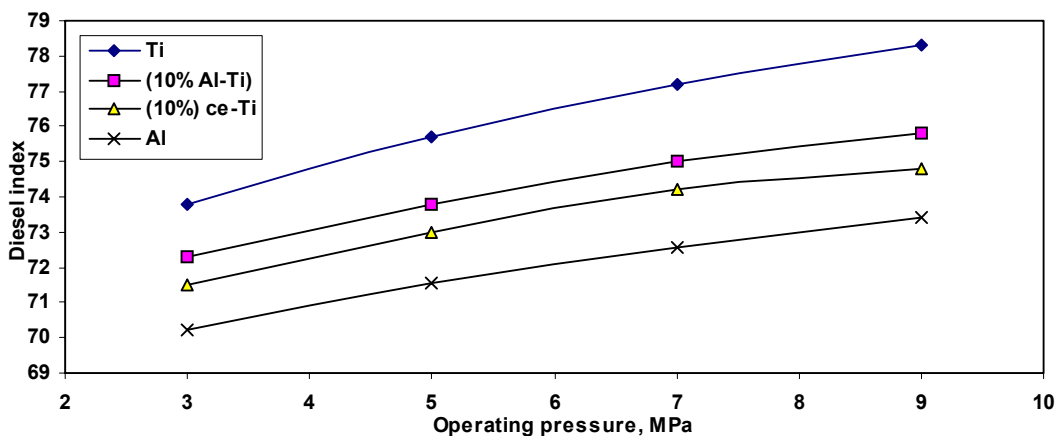


Fig. 20: Diesel index of diesel fuel product (210-348°C) as a function of operating pressure

(Temperature = 375°C, LHSV = 1.5 h⁻¹ and H₂/oil Ratio = 450 v./v.)

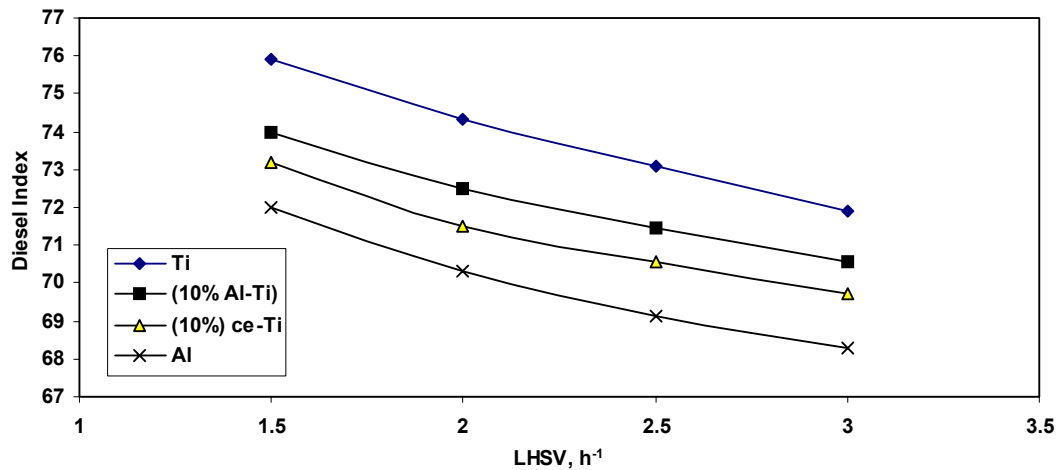


Fig. 21: Diesel index of diesel fuel product (210-348°C) as a function of LHSV

(Temperature = 375°C, operating pressure = 5.0 Mpa and H₂/oil Ratio = 450 v./v.)